

DUST AND IONIZED GAS IN NGC 3607¹K. P. SINGH,² T. P. PRABHU,³ A. K. KEMBAVI,⁴ AND P. N. BHAT²

Received 1993 May 10; accepted 1993 October 5

ABSTRACT

We report the detection of a broad dust ring in the X-ray-bright elliptical galaxy NGC 3607, the dominant member of a nearby group of galaxies. The inner radius of the ring is ~ 1.3 kpc from the nucleus and has a width of ~ 0.75 kpc. The maximum extinction corresponds to $E(B - V) = 0.12 \pm 0.023$. We also confirm the existence of bright H α nebulosity around the nuclear region of the galaxy, just inside the dust ring. The luminosity in H α is $\sim 1.5 \times 10^{40}$ ergs s⁻¹. The estimated amount of neutral hydrogen in the galaxy is $\sim 4 \times 10^7 M_{\odot}$ and ionized hydrogen $\sim 1.1 \times 10^5 M_{\odot}$. We rule out H α emission due to cooling flow, heat conduction from hot gas to the cold gas, photoionization by post-AGB stars or an active nucleus, and suggest that photoionization by young stars is the most plausible cause. We also suggest that the dust and associated gas are acquired from an interacting neighbor NGC 3608. The results are based on CCD surface photometry of the galaxy carried out using the broad-band filters *V* and *R* and a narrow-band filter appropriate for the redshifted H α + [N II] emission.

Subject headings: galaxies: elliptical and lenticular, cD — galaxies: individual (NGC 3607) — galaxies: ISM — radiation mechanisms: thermal — X-rays: galaxies

1. INTRODUCTION

Evidence for the presence of gas and dust in elliptical and lenticular galaxies has been accumulating for some time now. A rich variety of interstellar matter, at different temperatures, including X-ray halos, warm ionized gas, dust lanes, and neutral atomic hydrogen has been detected in many such galaxies. The existence of ionized material is particularly noticeable in the dominant galaxies of clusters with cooling flows (Heckman et al. 1989) but has also been documented in isolated ellipticals (Phillips et al. 1986; Shields 1991; Trinchieri & di Serego Alighieri 1991). The presence of dust often found in cooling flow galaxies has also been linked to galaxy-galaxy interactions (Forbes 1991). Despite a number of studies, it has not been possible to establish clearly the origin of dust and ionizing agents, particularly in the isolated ellipticals or in small groups. In order to improve our understanding of these systems, we are carrying out CCD observations of ionized gas and dust in elliptical galaxies which are in small groups and which have extended X-ray emission.

In this paper, we focus on a study of dust and gas in the elliptical galaxy NGC 3607. We have targeted this galaxy because it is the brightest member of its group (Vennik 1986), with two close neighbors, viz., NGC 3605 and NGC 3608 at a projected separation of about 2' and 5', respectively, and also because it is immersed in hot X-ray gas. It shows strong evidence for interaction with one of its neighbors, NGC 3608, which might have caused a distention of its envelope leading to its classification as S0 in some catalogs (Jedrzejewski & Schechter 1988). The general properties of this group, with redshift measurements for eight of its members, have been listed by Vennik (1986). The radial velocity of NGC 3607 is 934 km s⁻¹, very close to the unweighted mean of the group which

is 944 km s⁻¹. The velocity dispersion for the group is 245 km s⁻¹. The hot thermal gas detected in X-rays has a temperature corresponding to $kT \simeq 1.2$ keV and total X-ray flux of 6.2×10^{-13} ergs cm⁻² s⁻¹ as measured with the *Einstein Observatory* (Fabbiano, Kim, & Trinchieri 1992; Kim, Fabbiano, & Trinchieri 1992). NGC 3607 is a weak radio source and has been detected at both 1.46 GHz and 5 GHz (Hummel & Kotanyi 1985; Fabbiano, Gioia, & Trinchieri 1989), with the radio emission being most nuclear.

We adopt a value of 32 Mpc for the distance of NGC 3607 as listed by Fabbiano et al. (1992) corrected for Virgocentric flow ($H_0 = 50$ km s⁻¹ Mpc⁻¹ is assumed in this paper). At this distance an angular size of 10'' corresponds to ~ 1.55 kpc, and the size of the galaxy is ~ 46 kpc \times 23 kpc. The X-ray luminosity is 7.6×10^{40} ergs s⁻¹.

We present the details of observations in § 2, images and results of the isophotal analysis in § 3, and a discussion in § 4.

2. OBSERVATIONS

The galaxy was imaged using a GEC P8603 front-illuminated CCD at the prime focus of the 2.3 m Vainu Bappu Telescope (VBT) at Kavalur, on the night of 1993 January 19. The images were obtained through broad-band *V* and *R* filters with exposure times of 15 and 8 minutes, respectively. Additionally, a 30 minute exposure was obtained using a narrow-band filter centered at 6584 Å and having a bandwidth of 100 Å. The spectrophotometric standard Feige 56 (Stone 1977) in a neighboring region of the sky was observed just after the galaxy for calibrating the narrow-band filter data. The standard stars in the "dipper asterism" region of the open cluster M67 were observed just before the galaxy for calibrating the broad-band filter data. The details of the CCD camera and its standardization using the M67 star cluster have been reported by Bhat et al. (1990), Bhat et al. (1992), and Anupama et al. (1993). In brief, the image scale on the CCD is 0''.6 pixel⁻¹ at the f/3.25 prime focus of the VBT and the field of view is 5.7 \times 3.8 arcmin². The readout noise of the CCD is ~ 10 electrons, and the gain setting corresponds to ~ 4 electrons per

¹ Based on observations using Vainu Bappu Telescope, VBO, Kavalur.

² Tata Institute of Fundamental Research, Bombay 400 005, India.

³ Indian Institute of Astrophysics, Bangalore 560 034, India.

⁴ Inter-University Centre for Astronomy and Astrophysics, Pune 411 007, India.

CCD count (ADU) (Prabhu, Mayya, & Anupama 1992). The seeing was typically about 2"0 (FWHM), and the sky was photometric.

3. ANALYSIS AND RESULTS

3.1. Continuum Images

We analyzed the CCD images using standard tasks in the IRAF⁵ software package. The image frames and flat-field frames were bias subtracted using the bias frames obtained very close to the observations. The best flat fields obtained from the twilight and the dawn sky were used for flat-field corrections. To improve the signal-to-noise ratio and to reduce the pattern noise seen at very low levels in the images due to electronic interference noise, we employed an approximation of the Weiner filter using the fast Fourier transforms as explained in detail by Wampler (1992).

The shapes of the isophotes of the galaxies were analyzed using the ellipse-fitting program in the STSDAS⁶ software package (for details, see Jedrzejewski 1987). The areas around the stars were masked and excluded from the isophotal analysis. An ellipse of mean intensity starting with trial values of ellipticity, position angle, and ellipse center was fitted to a galaxy contour at a given length of the semimajor axis. The first two harmonics of the deviations from the trial ellipse were found. A minimum of 10 iterations, a maximum of 60, were performed to minimize the deviations and the best-fitted ellipse determined and its parameters calculated. The third and fourth harmonics of the residual intensity from the best-fitted ellipse were then evaluated by using the method of least squares. The procedure was repeated after increasing the semimajor axis length by 10%, taking annuli and using the median value of the pixels for sampling along the elliptical path. The ellipse center was held fixed during the fitting at a position obtained from trial fitting of the central regions without fixing the center. The errors on all the parameters of the ellipse were also evaluated. The procedure was repeated for the data from all the filters. We excluded the core region of the galaxy from the above analysis as these are affected by the seeing. The broad-band transformation equations were derived using nine stars in an M67 frame in the manner described by Anupama et al. (1993). The residual scatter was <0.02 mag in both *V* and *R* bands. The H α flux was estimated using Feige 56, with no correction being made for atmospheric extinction. The galaxy and the spectrophotometric standard were observed close to zenith whereas M67 was observed at an air-mass difference of $\Delta X = 0.1$. The range of extinction values observed at VBO during 1991 and 1992 (Mayya 1993) show that the effect of neglecting extinction would be <0.01 mag in colors and <0.05 on mag; the upper limits here are estimated using the maximum observed value for extinction during the two seasons.

In Figure 1, we show the surface brightness profile in the *V* band at the top and the ellipticity and the position angle profiles obtained from the above analysis at the bottom. Results from both the *V* and *R* images are displayed together for the ellipticity the position angle profiles and are in agreement. The isophotal analysis shows a depression in the surface brightness profile between 8" and 15". Sharp features are visible near this

region in the ellipticity and position angle profiles. The ellipticity is higher than average between 6" and 8" and sharply lower around 15", and the position angle profile shows kinks at precisely the same locations in the galaxy. These positions correspond to the inner and outer edges of the dust ring seen in the color map (see § 3.2 below). In general, the cosine coefficient of the fourth harmonic (plotted in Fig. 2) is an indicator of the hidden structure of the galaxy (positive for "boxy" and negative for "disk" structure) and has been found to correlate with the strength of radio emission and the presence of hot thermal gas (Bender et al. 1989). It shows a very irregular behavior here.

We have derived the half-light radius r_e by fitting a de Vaucouleurs profile to the surface brightness profile shown in Figure 1 after converting the *x*-axis to an effective radius given by $(ab)^{0.5}$, where *a* and *b* are the semimajor and semiminor axes, respectively. We ignored the central regions of the galaxy affected by seeing and dust. The value of r_e thus obtained is $\approx 6 \pm 0.2$ kpc. This value lies between the two estimates by Bender et al. (1989) and Bender, Burstein, & Faber (1992) who, adopting a distance of ~ 20 Mpc, derive r_e of 2.45 kpc in their 1989 paper and 6.4 kpc in their 1992 paper, which correspond to 4 kpc and 10.3 kpc, respectively, for the 32 Mpc distance assumed here.

3.2. Color Map and Dust Rings

We created a color map of NGC 3607 by dividing the *V* image by the *R* image after flat-field corrections, sky subtraction, and alignment of stars in the images. The alignment shift was less than 2 pixels in the *x*- and *y*-directions of the frame, and the *R* frame was linearly interpolated. The color map thus obtained is shown in Figure 3 (Plate 17) with darker areas corresponding to redder color. An increased reddening is visible in a broad ringlike structure with inner and outer radii of approximately 8"4 and 13"2, respectively. It is precisely the inner and outer edges of this feature that led to the bumps in the profiles shown in Figure 1. The color also shows a sharp gradient along the northeastern edge of the ring and a shallower gradient on the diametrically opposite side. A few sharper features or ringlets are also visible inside the broader reddened feature. We interpret these observations to be indicators of dust confined to rings in a disk that is tilted forward in the northeastern side. The nucleus of the galaxy appears to be relatively bluer, and some of the ringlets appear to spiral into the nucleus.

The instrumental magnitudes obtained from the *v/r* color map when translated to the standard (*V* - *R*) color yielded

$$V - R = 0.662 \pm 0.013 \text{ (inside the ring) ,}$$

$$V - R = 0.568 \pm 0.013 \text{ (just outside the ring) .}$$

The color then slowly drops off to the value $V - R = 0.550 \pm 0.010$ in the outer parts of the galaxy. Therefore, the extinction in the broad dust ring is

$$E(V - R) = 0.094 \pm 0.018 ,$$

and using the relations given in Savage & Mathis (1979), we obtain

$$E(B - V) = 0.120 \pm 0.023 .$$

We estimate the effective optical depth in *V* and *R* bands by summing data along five columns as a function of lines, by estimating the starlight from a smooth interpolation around

⁵ IRAF is distributed by the National Optical Astronomy Observatories, which is operated by the Association of Universities, Inc. (AURA) under cooperative agreement with the National Science Foundation.

⁶ The Space Telescope Science Data Analysis System (STSDAS) is distributed by the Space Telescope Science Institute.

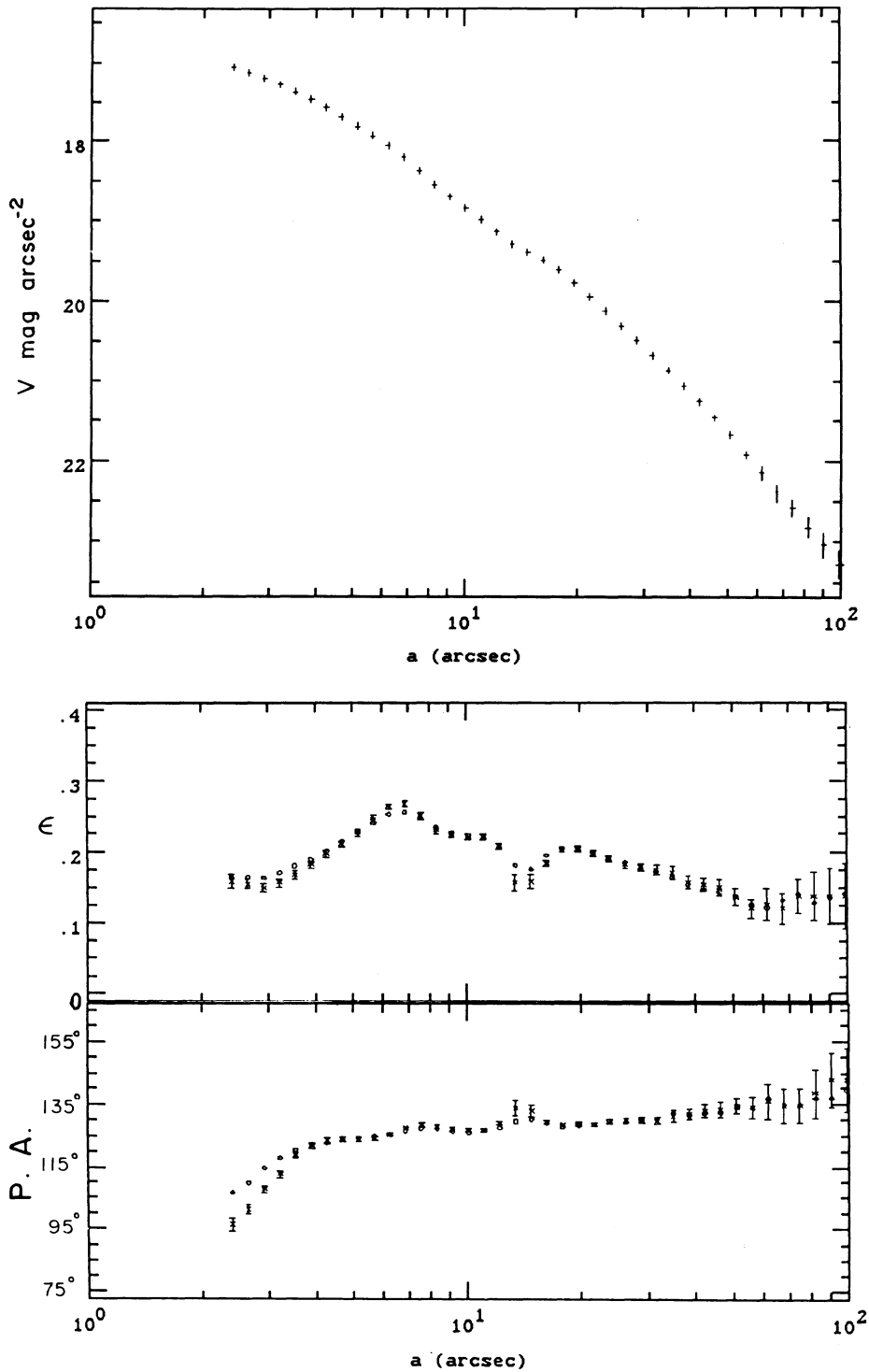


FIG. 1.—Surface brightness profile of NGC 3607 in the V band as a function of the semimajor axis in arcseconds is shown at the top. The brightness is in units of mag arcsec^{-2} . The ellipticity and position angle profiles along the semimajor axis, derived from the V and R images, are also shown (crosses for V and open circles for R). The position angle may have a systematic error of $\sim 5^\circ$.

the dust region, and dividing the observed counts by the interpolated values. We carried out this exercise for five regions in the galaxy. A plot of a few regions from the V band data showing a dip due to extinction is given in Figure 4. Converting the above values to extinction A_v and A_r , for V and R frames respectively, we find a value of ~ 0.76 for the ratio of

A_r/A_v which is similar to the value of 0.77 determined in our Galaxy. The dust properties are, therefore, similar to that in our Galaxy, and the covering factor of dust is large as derived by Sparks, Macchetto, & Golombek (1989) in the case of NGC 4696. Thus we can use the approximation of sheetlike geometry for the dust layer obscuring the starlight.

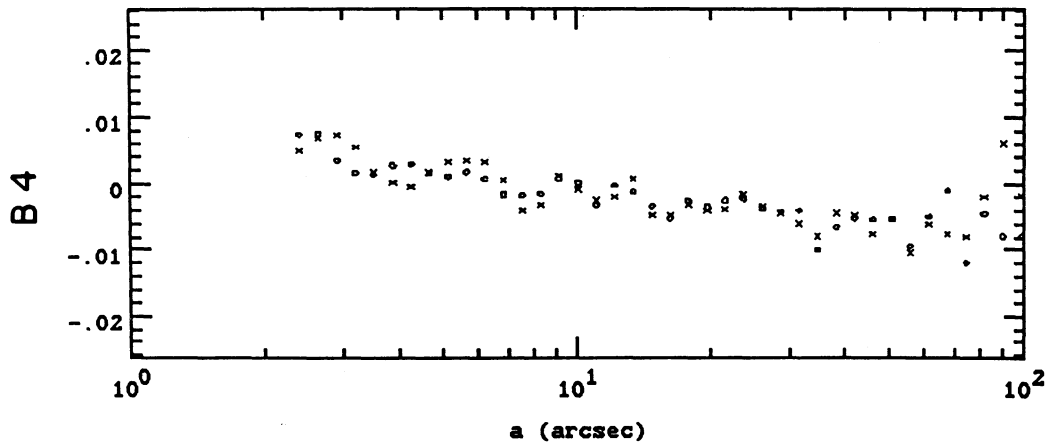


FIG. 2.—The cosine coefficient of the fourth harmonic as a function of the semimajor axis in arcseconds of NGC 3607

3.3. $H\alpha + [N II]$ Emission

The image of the galaxy in the $H\alpha + [N II]$ line emission was obtained by subtracting the continuum image in the R filter, after proper scaling and realignment, from the image taken with the narrow-band filter. The scaling factor was estimated from the relative efficiencies of the narrow-band filter and R filter, derived from the observations of the spectrophotometric standard Feige 56, and assuming that the stellar component in the galaxy has a similar spectrum. The resultant surface brightness of the line emission is shown in Figure 5 in a contour plot. The $H\alpha + [N II]$ emission is concentrated around the nuclear region but is clearly resolved; it is extended with an elliptical distribution with higher eccentricity but the same position angle as the continuum. The size of the line emission region places it just inside the dust ring. The total $H\alpha + [N II]$ luminosity is found to be 4.3×10^{40} ergs s^{-1} . Assuming a mean value of 1.38 for $[N II]\lambda 6583/H\alpha$ (Phillips et

al. 1986), and the ratio of 3 for $\lambda 6583/\lambda 6548$ we obtain a corrected $H\alpha$ luminosity of 1.5×10^{40} ergs s^{-1} .

The foreground extinction to NGC 3607 due to our Galaxy is negligible (Burstein & Heiles 1984). The effect of foreground dust in NGC 3607 can be estimated if $H\beta$ flux is also available. If the reddening of $H\alpha$ is similar to that in the dust ring, we will need to increase the observed emission flux by 30%. Since the exact amount of reddening suffered by emitting gas is unknown at present, we will neglect this in the following.

4. DISCUSSION

The present observations have detected dust rings and confirmed the existence of $H\alpha$ line emission in NGC 3607. Both dust and $H\alpha$ nebulosities are commonly found in cooling flow galaxies, but their presence does not necessarily imply the existence of a cooling flow (see Forbes 1991). The existing X-ray

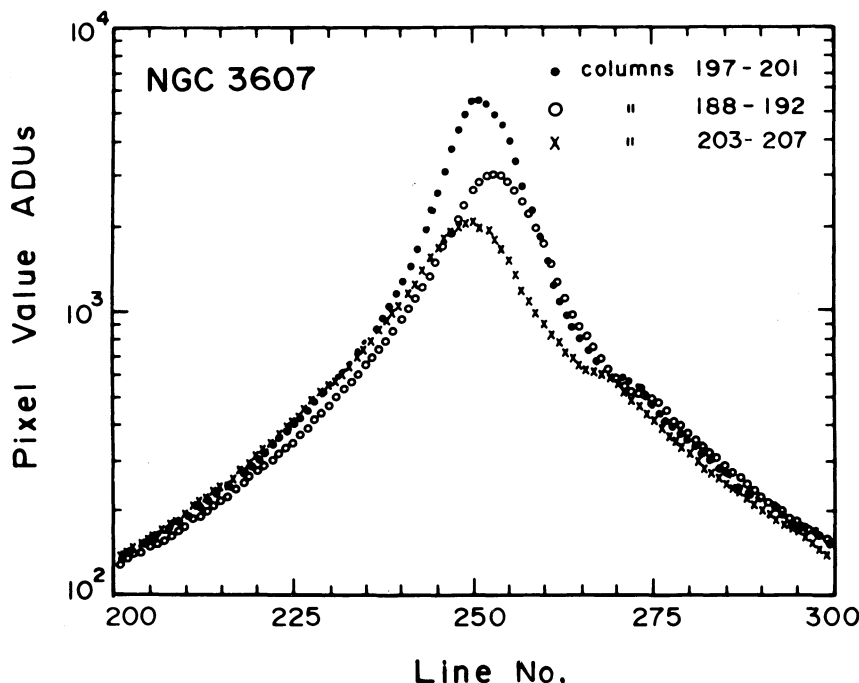


FIG. 4.—Linear plots along lines in the CCD from different groups of five columns summed together. The dip in the data is clearly visible on one side.

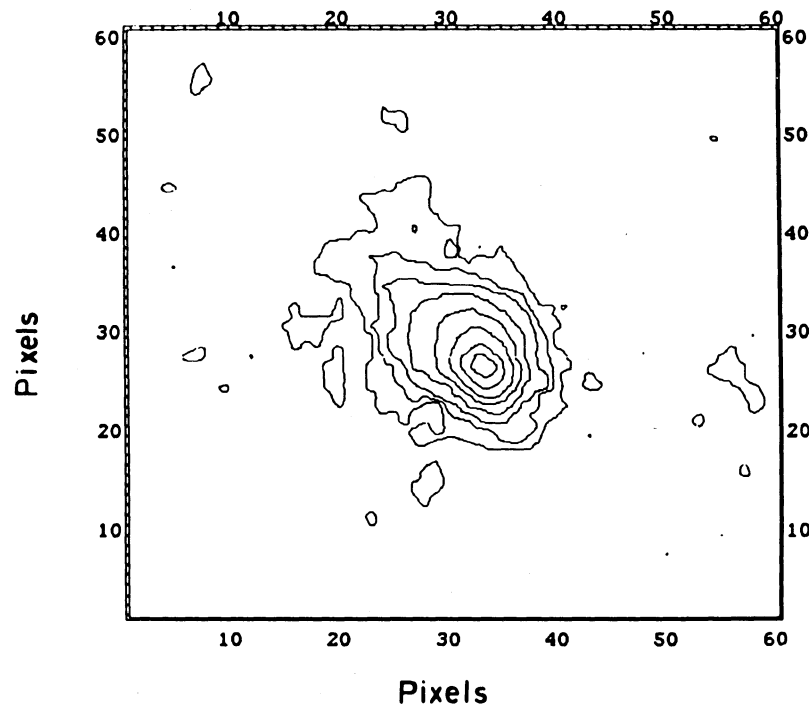


FIG. 5.—Contour plot of H α image of NGC 3607. The image size shown here is $36'' \times 36''$. The contour levels, expressed in units of 10^{-16} ergs cm^{-2} s^{-1} arcsec^{-2} , are 3.8, 9.6, 15.4, 26.9, 44.2, 67.3, 101.9, and 136.5 after correcting for the median sky value. East is up, and north is the the right (approximately).

observations did not have sufficient resolution to detect any cooling flow in this galaxy. The lack of detailed correlations among the various indicators of cooling flow in a sample of ellipticals does not strongly favor the cooling flow origin of gas and dust and suggests alternative external origin (Forbes 1991). In the following, we discuss in detail various ionization mechanisms that are likely to produce the warm ionized gas and the origin of the dust.

4.1. Dust and Neutral Gas

The existence of dust implies that there must be a mechanism to protect it from the hot gas that can thermally sputter the dust (Draine & Salpeter 1979). It is likely that the dust is embedded in clouds of neutral gas and survives evaporation due to shielding by tangled magnetic fields that can suppress the heat conduction (Stewart et al. 1984), as has been suggested previously (e.g., for M84 by Hansen, Norgaard-Nielsen, & Jorgensen 1985).

We estimate the amount of neutral gas as follows. Assuming that the gas is distributed homogeneously (see § 3.2) and that the dust-to-gas ratio is similar to that in our Galaxy (Savage & Mathis 1979), we have

$$N(\text{H I})/E(B-V) = 5.0 \times 10^{21} \text{ atoms cm}^{-2} \text{ mag}^{-1}$$

(Burstein & Heiles 1978). This gives, for the value of $E(B-V)$ derived in § 3.2,

$$N(\text{H I}) = 6 \times 10^{20} \text{ atoms cm}^{-2}.$$

For the observed ring (inner and outer radii of ~ 1.3 and 2.0 kpc, respectively; see § 3.2), this implies a total mass of $4 \times 10^7 M_{\odot}$ for H I in the ring. One would hence expect an integrated flux in the 21 cm H I line of $0.165 \text{ Jy km s}^{-1}$. The current limit on this flux is $3.26 \text{ Jy km s}^{-1}$ (Knapp, Turner, & Cunniffe 1985), although in better observations, an integrated flux of

$0.21 \text{ Jy km s}^{-1}$ has been detected in the neighboring galaxy NGC 3608.

4.2. Ionized Gas

Optical nebulosity from NGC 3607 was first imaged by Shields (1991). We have compared our results with those presented earlier by using the same value of the distance and aperture size and by performing aperture photometry using the DAOPHOT package developed by Stetson (1987). The total line flux for an aperture radius of 2 kpc is thus calculated to be 2.3×10^{40} ergs s^{-1} which is in excellent agreement with the value given by Shields (1991). The line images, however, differ slightly in the overall shape possibly due to differences in the point-spread functions.

Phillips et al. (1986) obtained values of electron density ranging from 170 to 410 cm^{-3} in a sample of eight cooling flow galaxies using the [S II] line ratios. Assuming a mean value of $N_e = 300 \text{ cm}^{-3}$ and electron temperature $T_e = 10^4 \text{ K}$ for NGC 3607, together with the observed size of the emitting region which indicates it could be a disk of radius 1.5 kpc and thickness of 200 pc, we obtain a filling factor of 1.1×10^{-5} using emissivities listed by Osterbrock (1989, case B). This value is within the range derived by Phillips et al. (1986). From the observed temperature of the X-ray gas, the emissivity of the hot plasma is $\approx 5 \times 10^{-23} \text{ erg cm}^{-3} \text{ s}^{-1}$ (Raymond, Cox, & Smith 1976). Assuming that the observed L_x is from the complete volume of the ellipsoidal galaxy, the average electron density is found to be $7 \times 10^{-4} \text{ cm}^{-3}$. The central density of the hot gas in which the optical line emission arises could be higher by an order of magnitude. Under the assumption of a pressure equilibrium between the warm gas (10^4 K) and hot (10^7 K) gas, we derive a value of 7 cm^{-3} for the H α gas density. This value of density implies a filling factor of ~ 0.02 . The total mass of the warm gas would be $5.0 \times 10^6 M_{\odot}$ for $N_e = 7 \text{ cm}^{-3}$ and $1.1 \times 10^5 M_{\odot}$ for $N_e = 300 \text{ cm}^{-3}$ with the corresponding

filling factors as derived above. We will present in § 4.4 below arguments for favoring the latter set of values.

4.3. Ionization Mechanism

4.3.1. Cooling Flow

As already pointed out above, cooling flow has not been detected so far in NGC 3607, the higher resolution and higher sensitivity X-ray observations are needed to establish its presence or absence. Since line emission is an indicator of the probable existence of cooling flow, we examine the hypothesis that the line emission is due to recombination of the cooling gas. The mass deposition rate due to cooling can be estimated from $\dot{m} = 2\mu m_H L_x / 5kT$, where L_x is the central excess X-ray luminosity, T is the temperature of the gas at the boundary of the cooling region, and μ is the mean molecular weight of the gas (Fabian, Nulsen, & Canizares 1991). Assuming $T = 10^7$ K, and that no more than 50% of the L_x comes from the cooling region we obtain an $\dot{m} = 0.5 M_\odot \text{ yr}^{-1}$, which is similar to that found in many ellipticals (Thomas et al. 1986). Considering that recombination of the cooling gas can produce $L_{\text{H}\alpha} \simeq 10^{37} \dot{m} \text{ ergs s}^{-1}$, where \dot{m} is in units of $M_\odot \text{ yr}^{-1}$ (Johnstone, Fabian, & Nulsen 1987), and assuming $F(\text{H}\alpha)/F(\text{H}\beta) = 2.8$ (case B, Osterbrock 1989), we expect $L_{\text{H}\alpha} \simeq 1.4 \times 10^{37} \text{ ergs s}^{-1}$ which is at least 10^3 smaller than the observed value. This result is consistent with the finding of Trinchieri & di Serego Alighieri (1991) for many other ellipticals, and follows the general trend seen by Johnstone et al. in many cooling flows. The observed H α emission requires either a very high recombination rate or a different ionization mechanism.

4.3.2. Photoionization by Stars

The emission-line gas could be photoionized by stars. The minimum number of Lyman-continuum photons Q (photons s^{-1}) required to produce the observed H α luminosity is $7.5 \times 10^{11} L_{\text{H}\alpha} \text{ (ergs s}^{-1}\text{)}$ (case B, Osterbrock 1989). This implies $Q = 1.1 \times 10^{52} \text{ photons s}^{-1}$. A population of hot, young stars can supply these photons. Johnstone et al. (1987) show that there is an indication in the optical spectra for the presence of young stars in many elliptical galaxies with emission-line nebulosities, and that the mass deposition and consequent star formation in cooling flow galaxies is consistent with the observed line emission. Good signal-to-noise ratio optical spectra are needed to check whether this applies to NGC 3607.

Ionizing radiation for an IMF with a slope of 2.5, a lower cutoff at $1 M_\odot$, and upper cutoff at $60 M_\odot$ is $3 \times 10^{46} \text{ photons s}^{-1} M_\odot^{-1}$ (Mayya 1993). The total mass in the young stars needed to explain the observed H α emission is then found to be $4 \times 10^5 M_\odot$. The e -folding time for ionizing radiation (due to evolution of the burst) is $5.5 \times 10^6 \text{ yr}$. Hence either we are seeing a young burst at the present epoch or the radiation is present all through and continuous star formation with a rate of $\sim 0.1 M_\odot \text{ yr}^{-1}$ is needed. If the total H I mass in the emission region is of the same order as the amount estimated for the dust ring (§ 4.1), one derives the present star formation efficiency of $\sim 1\%$, which appears reasonable. Continuous star formation with the current rate would then require an infall of $10 M_\odot \text{ yr}^{-1}$. This rate is much higher than expected from a cooling flow on the one hand, and on the other, cooling flows fall short of explaining the emission even with such a large infall rate. We consider this a strong argument for an external origin of the gas and ionization due to star formation.

An alternative possibility is ionization by the post-

asymptotic giant branch (PAGB) stars (Trinchieri & di Serego Alighieri 1991). These stars spend about 10^5 yr at surface temperatures between 3×10^4 and 10^5 K at luminosities ranging from 3×10^3 to $10^4 L_\odot$ (Renzini & Buzzoni 1986). Assuming that these objects radiate like blackbodies, we estimate a mean value of $Q = 5 \times 10^{46} \text{ photons s}^{-1}$ for each PAGB star. Thus we need to have $\sim 10^6$ such stars to explain the observed H α emission. The fact that the gas is clumpy and the covering factor is likely to be low makes this value a lower limit. For a total galactic luminosity of $\sim 10^{10} L_\odot$ within the emitting region one expects at most $\sim 10^5$ such stars at any given epoch (Renzini & Buzzoni 1986). We therefore conclude that the mechanism is not a likely source of ionization in the case of NGC 3607.

4.3.3. Heat Conduction

It has been suggested that heat transfer from the hot gas to cool gas may provide sufficient energy for the excitation of optical emission lines in NGC 4694 in the Centaurus cluster, which also contains a prominent dust lane (Sparks et al., 1989). Using expression (19) of Sparks et al. for the saturated heat flow and scaling the temperature, density, and area appropriately to NGC 3607, we find that the heat flow is $\sim 6 \times 10^{40} \text{ ergs s}^{-1}$. A comparison of the emissivity at 10^4 K by Raymond et al. (1976) and Osterbrock (1989) shows that the total radiation due to line emission from the warm gas at 10^4 K may be about ~ 20 times the cooling rate in H α + [N II]. Therefore, the cooling rate of the warm gas is $8 \times 10^{41} \text{ ergs s}^{-1}$, which is more than what can be supplied through heat transfer (we have neglected any cooling of dust due to infrared radiation as none has been detected so far). Hence, heat transfer through conduction cannot work in the present example; other elliptical galaxies in the sample of Trinchieri & di Serego Alighieri (1991) will also have a similar problem. Apart from energetics, the presence of dust in the galaxy suggests that heat transfer through conduction cannot be very strong.

4.3.4. Nuclear Activity

It is possible that the H α nebulosity close to the nucleus is related to the presence of nonthermal activity in the nucleus. The blue color of the nucleus and nuclear radio emission do indeed point toward a mild activity, but processes associated with nuclear activity have generally been shown to be inadequate by Heckman et al. (1989). High-resolution spectroscopy is required to confirm nuclear activity, but it is clear that a good part of the extended H α emission must originate due to other causes.

4.4. Accretion from NGC 3608

A study of the absorption-line kinematics in NGC 3608, a neighbor of NGC 3607, has provided evidence for a close encounter between the two galaxies (Jedrzejewski & Schechter 1988). It has been suggested that the interaction has resulted in a torque on the outer parts of NGC 3608, which reverses the sense of rotation of some stars in that region. NGC 3607 may have captured some of the loosely bound stars of NGC 3608, thus contributing to its extended envelope. Because of the close encounter, accretion of gas and dust from NGC 3608, where H I has been detected (Knapp et al. 1985), is likely to be taking place. The dust and gas in NGC 3607 are hence likely to be a recent acquisition and of an external origin, consistent with the general picture of Forbes (1991).

If we assume that the accreted cold H I clouds—instead of

the warm H II clouds—are in pressure equilibrium with the hot gas, we obtain a density of 700 cm^{-3} for clouds of temperature 100 K. The filling factor at this density $\sim 1.5 \times 10^{-3}$ in the disk. Since the filling factor is approximately the size of the cloud divided by the total column length, we obtain the mean size of the clouds to be ~ 2 pc. Typical masses of these clouds would then be $\sim 20 M_{\odot}$. We expect $\sim 10^6$ such clouds in the dust ring and a similar number in the line emission region. The lower filling factor for the line-emitting gas would then imply that the star formation has taken place in $\sim 10^3$ of these clouds. One expects a distribution of cloud masses and sizes in a realistic situation which may lead to star formation preferentially in larger clouds. Even so, the estimate of $4 \times 10^5 M_{\odot}$ in young stars marginally agrees with the total mass in star-forming clouds. The discrepancy can be resolved if the stars form in OB associations which lack low-mass stars. Such top-heavy star formation has been suggested in the case of starburst galaxies (Scalo 1990).

Finally one may conjecture that the pressure due to the hot gas provides the necessary compression triggering the star formation event as the clouds from NGC 3608 sink into the hot gas centered at NGC 3607.

5. CONCLUSIONS

1. We have reported here our discovery of dust rings at radial distance of 0.75–1.3 kpc in NGC 3607. The dust has the

“standard” properties observed in our Galaxy. The associated neutral hydrogen should have a mass of $4 \times 10^7 M_{\odot}$, and we expect 21 cm line flux of $0.17 \text{ Jy km s}^{-1}$.

2. We confirm significant amount of H α emission originating in the region just interior to the dust ring. Cooling flow recombination, heat transfer from hot (X-ray-emitting) gas to the warm (H α -producing) gas, and ionization by post-AGB stars or an active nucleus, fall short of explaining the observed H α luminosity. On the other hand, ongoing star formation at the present time can provide the ionizing photons needed to explain the H α emission but requires $\sim 10 M_{\odot} \text{ yr}^{-1}$ to be injected.

3. Infall is needed to supply “standard dust” to the galaxy, and a suitable companion and supplier is NGC 3608. The two galaxies present evidence for recent interaction. It appears that the star formation is triggered in clouds acquired from NGC 3608 as they sink into the hot gas centered around NGC 3607.

We are grateful to the staff of Indian Institute of Astrophysics, Bangalore for the maintenance of the CCD system. We thank G. Selvakumar and M. Ganesan for their assistance during the observations.

REFERENCES

- Anupama, G. C., Kembhavi, A. K., Prabhu, T. P., Singh, K. P., & Bhat, P. N. 1993, *A&AS*, in press
 Bender, R., Burstein, D., & Faber, S. M. 1992, *ApJ*, 399, 462
 Bender, R., Surma, P., Dobreiner, S., Mollenhoff, C., & Madejsky, R. 1989, *A&A*, 217, 35
 Bhat, P. N., Kembhavi, A. K., Patnaik, K., Patnaik, A. R., & Prabhu, T. P. 1990, *Indian J. Pure & Appl. Phys.*, 28, 649
 Bhat, P. N., Singh, K. P., Prabhu, T. P., & Kembhavi, A. K. 1992, *J. Astrophys. Astron.*, 13, 293
 Burstein, D., & Heiles, C. 1978, *ApJ*, 225, 40
 ———. 1984, *ApJS*, 54, 33
 Draine, B. T., & Salpeter, E. E. 1979, *ApJ*, 231, 77
 Fabbiano, G., Gioia, I. M., & Trinchieri, G. 1989, *ApJ*, 347, 127
 Fabbiano, G., Kim, D.-W., & Trinchieri, G. 1992, *ApJS*, 80, 531
 Fabian, A. C., Nulsen, P. E. J., & Canizares, C. R. 1991, *Astron. Astrophys. Rev.*, 2, 191
 Forbes, D. A. 1991, *MNRAS*, 249, 779
 Hansen, L., Norgaard-Nielsen, H. U., & Jorgensen, H. E. 1985, *A&A*, 149, 442
 Heckman, T. M., Baum, S. A., van Breugel, W. J. M., & McCarthy, P. 1989, *ApJ*, 338, 48
 Hummel, E., & Kotanyi, C. G. 1985, *A&A*, 145, 475
 Jedrzejewski, R. I. 1987, *MNRAS*, 226, 747
 Jedrzejewski, R., & Schechter, P. L. 1988, *ApJ*, 330, L87
 Johnstone, R. M., Fabian, A. C., & Nulsen, P. E. J. 1987, *MNRAS*, 224, 75
 Kim, D.-W., Fabbiano, G., & Trinchieri, G. 1992, *ApJS*, 80, 645
 Knapp, G. R., Turner, E. L., & Cunniffe, P. E. 1985, *AJ*, 90, 454
 Mayya, Y. D. 1993, PhD thesis, Indian Institute of Science, Bangalore
 Osterbrock, D. E. 1989, *Astrophysics of Gaseous Nebulae and Active Galactic Nuclei* (Mill Valley, CA: University Science Books)
 Phillips, M. M., Jenkins, C. R., Dopita, M. A., Sadler, E. M., & Binette, L. 1986, *AJ*, 91, 1062
 Prabhu, T. P., Mayya, Y. D., & Anupama, G. C. 1992, *J. Astrophys. Astron.*, 13, 129
 Raymond, J. C., Cox, D. P., & Smith, B. W. 1976, *ApJ*, 204, 290
 Renzini, A., & Buzzoni, A. 1986, in *Spectral Evolution of Galaxies*, ed. C. Chiosi & A. Renzini (Dordrecht: Reidel), 195
 Savage, B. D., & Mathis, J. S. 1979, *ARA&A*, 17, 73
 Scalo, J. 1990, in *Windows on Galaxies*, ed. G. Fabbiano, J. S. Gallagher, & A. Renzini (Dordrecht: Kluwer), 125
 Shields, J. C. 1991, *AJ*, 102, 1314
 Sparks, W. B., Macchetto, F., & Golombek, D. 1989, *ApJ*, 345, 153
 Stetson, P. B. 1987, *PASP*, 99, 191
 Stewart, G. C., Canizares, C. R., Fabian, A. C., & Nulsen, P. E. J. 1984, *ApJ*, 278, 536
 Stone, R. P. S. 1977, *ApJ*, 218, 767
 Thomas, P. A., Fabian, A. C., Arnaud, K. A., Forman, W., & Jones, C. 1986, *MNRAS*, 222, 655
 Trinchieri, G., & di Serego Alighieri, S. 1991, *AJ*, 101, 1647
 Vennik, J. 1986, *Astr. Nachr.*, 307, 157
 Wampler, E. J. 1992, *ESO Messenger*, 70, 82

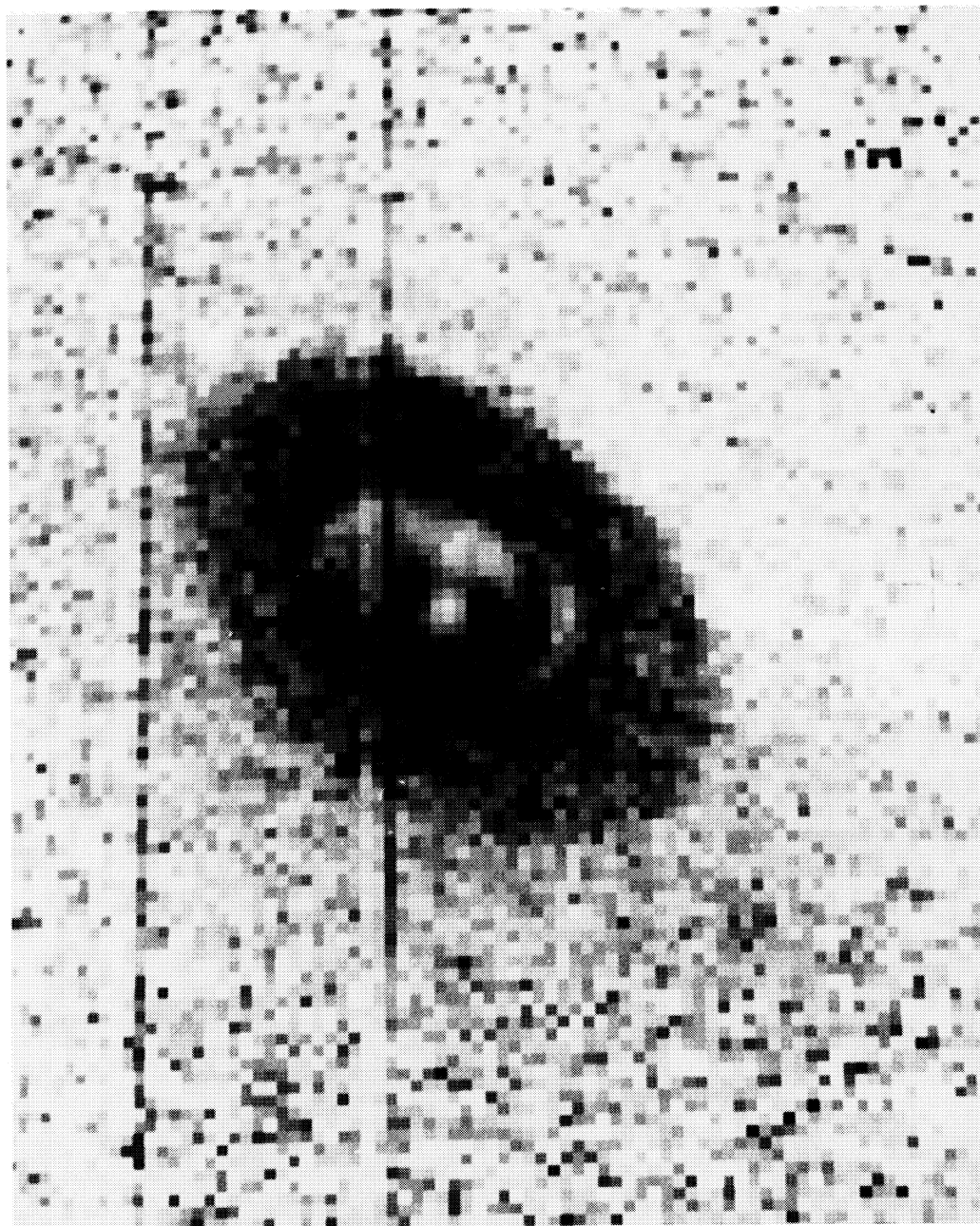


FIG. 3.—*V/R* color map of NGC 3607. The redder regions are shown darker. The size of the image is $\sim 60'' \times 45''$. East is up, and north is to the right (approximately).

SINGH, PRABHU, KEMHAVI, & BHAT (see 424, 639)